arXiv:1604.02453v1 [cond-mat.mtrl-sci] 10 Apr 2016

A critical assessment of models of pair-interactions and screening used in analyzing recent warm-dense matter experiments.

L. Harbour,[1] M. W. C. Dharma-wardana,[2] D. D. Klug,[2] and L. J. Lewis[1]

[1] *Département de Physique and Regroupement Québécois sur les Matériaux de Pointe, Université de Montréal, C.P. 6128, Succursale Centre-Ville, Montréal, Québec, Canada H3C 3J7*

[2] *National Research Council of Canada, Ottawa, On., Canada K1A 0R6**

(Dated: April 12, 2016)

Ultra-fast laser experiments yield increasingly reliable data on warm-dense matter (WDM), but rely on entrenched simplistic theoretical models. We re-analyze two topical experiments, avoiding (i) *ad hoc* core-repulsion models, (ii) "Yukawa screening" models and (iii) electron-ion equilibrium assumptions. An accurate, rapid density-functional neutral-pseudoatom model coupled to a hyper-netted-chain (HNC) equation with a bridge term is used to compute structure factors, X-Ray scattering, compressibility, phonons and resistivity. Electronic-structure codes are used to confirm the calculations. The Yukawa and core-repulsion models are shown to be misleading.

Introduction– High-energy deposition using ultra-fast lasers has created novel non-equilibrium regimes of density and temperature, raising issues of broad scientific interest. The topics cover hollow atoms, quasi-solids and transient plasmas. The physics of such warm-dense matter (WDM) applies to hot-carriers in nanostructures, space re-entry, protective shields against photonic weapons, inertial confinement fusion [1, 2], Coulomb explosions, laser machining and ablation [3], and in astrophysics. WDM systems are strongly-correlated, with the effective coupling parameter Γ (ratio of the Coulomb energy to the kinetic energy) greatly exceeding unity.

WDM systems are created using, e.g., (i) shock-compression [4–6] and (ii) ultra-fast laser heating [7–9]. In ultra-fast heating the femto-second optical pulses directly heat the electrons, increasing their temperature T_e to many eV, while the ions remains nearly at their initial temperature and density ρ^0. Such WDM systems are referred to as ultra-fast matter (UFM). At short time scales (e.g., <100 fm) even the electrons may not equilibrate to a temperature [10]. The ions and electrons equilibrate in timescales exceeding the electron-ion relaxation time τ_{ei}, i.e., over hundreds of picoseconds [8, 11]. Thus, experiments with $t < \tau_{ei}$ deal with non-equilibrium UFM. The simplest non-equilibrium paradigm is the well-known two-temperature ($2T$) model [12]. Nevertheless, many WDM-UFM studies have used equilibrium models, although later shown to need at least a $2T$ model [13–15]. Electronic-structure codes [16, 17] based on density functional theory (DFT) coupled with molecular dynamics (MD) are used for interpreting these experiments.

The results from DFT-MD have themselves been fitted to intermediate quantities like pair-potentials to harvest more physics and simplify the computations. Simple intuitive models usually have hidden pitfalls that become entrenched unless corrected. The objective of this study is to re-analyze two recent experiments [4–6] using the DFT neutral-pesudo-atom(NPA) approach which is as accurate as the DFT-MD codes for many systems, but orders of magnitude faster. It directly yields physically useful quantities like pair potentials and structure factors needed in computing observed properties.

Many WDM studies during the last seven years, e.g., in Refs.[4, 6] have used an intuitive "Yukawa + short-ranged repulsive (YSRR) potential" $\beta_i V_{ii}^{\rm ysrr}(r) = \sigma^4/r^4 + \beta_i \exp(k_s r)/r$ introduced in Ref. [20]. $T_i = 1/\beta_i$ is the ion temperature, k_s is a screening wavevector and σ is a parameter fitted to MD data. We examine its validity using first-principles models and XRTS data for ultrafast ($T_e \neq T_i$) as well as equilibrium systems. The YSRR potential is found to produce misleading conclusions.

XRTS data yields T_e, T_i, ion density ρ, electron density n_e, and details of ionic and electronic correlations. An important component of the XRTS signal is the *ion feature* $W(k)$. [21, 22]

$$W(\mathbf{k},\omega) = |f(\mathbf{k}) + q(\mathbf{k})|^2 S_{ii}(\mathbf{k},\omega) \quad (1)$$

$$S_{ii}(\mathbf{k},\omega) \simeq S_{ii}(\mathbf{k})\delta(\omega) \quad (2)$$

Here $f(\mathbf{k})$ and $q(\mathbf{k})$ are the form factors of bound and free electron densities at an ion. $S_{ii}(\mathbf{k},\omega)$ is the dynamic structure factor of the ions. Current XRTS cannot resolve ion dynamics (at meV energy scales). It is approximated via the static structure factor $S_{ii}(k)$, denoted hereafter as $S(k)$.

An XRTS $W(k)$ calculation needs the electron densities at an ion, and the $S(k)$ of the system. The NPA approach [23, 24] decomposes the total charge density into a superposition of effective one-body charge densities and structure factors, and provides a comprehensive scheme based on DFT. A number of NPA models are described in the literature, e.g., those using ion-sphere models and other prescriptions. These affect how the chemical potential is treated, and how the bound and free electrons are identified[25, 26]. We use the NPA model of Perrot and Dharma-wardana [25, 27] which uses a large "correlation sphere" of radius $R_c \sim 10 r_{ws}$, where $r_{ws} = \{3/(4\pi\rho)\}^{1/3}$ is the ion Wigner-Seitz radius. The electron chemical potential is that of non-interacting electrons at the interacting density n_e at T_e, as required by DFT. This model

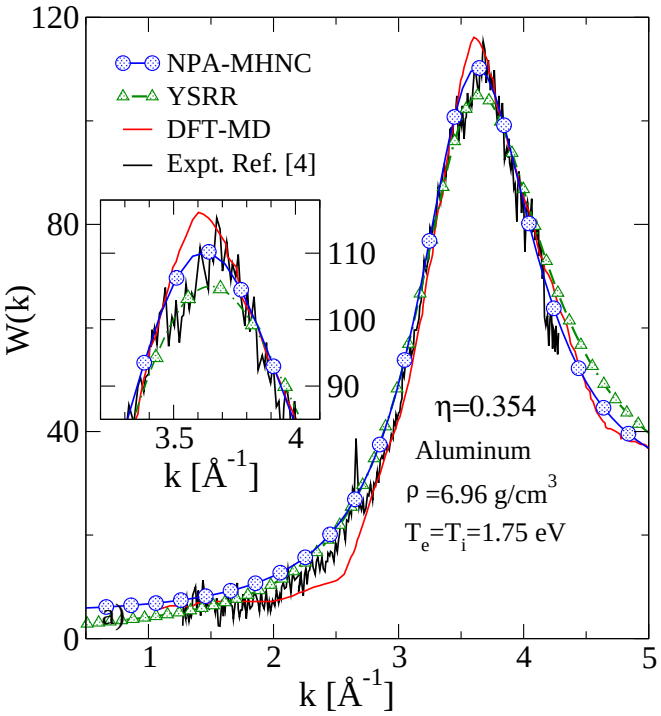

FIG. 1: The XRTS ion feature $W(k)$ of Ref. [4], and from DFT+MD, NPA-MHNC and YSRR models.

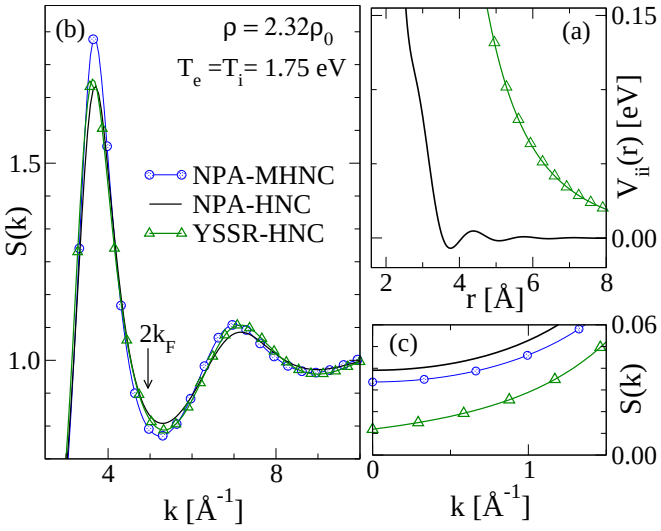

FIG. 2: (a)NPA and YSRR potentials. (b) $S(k)$ from the $V_{ii}(r)$, using HNC and MHNC. (c) $k \to 0$ region of $S(k)$.

accurately predicts phonons (i.e., meV accuracy) in $2T$ WDM systems [28]. Thus even the dynamical $S_{ii}(\mathbf{k},\omega)$ can be predicted when XRTS data at meV accuracy become available.

Study of WDM-Al by Fletcher et al– Fletcher *et al* [4] have studied compressed aluminum evolving across the melting line into a WDM state, using XRTS. The data can be used to extract $S_{ii}(k)$, the temperatures, compressibilities, pseudo-potentials etc., and transport properties like the conductivity. While DFT+MD can provide numerical results up to moderate T, such simulations fall short on clarifying the physics. The physics comes out clearly in the DFT-NPA method [29], avoiding misleading *ad hoc* YSRR-type models.

The use of an equilibrium ($T_e = T_i$) model by Fletcher *et al* is justifiable for nano-second time sacles. The NPA calculation provides the free-electron charge density $n_f(r)$ at an Al^{3+} ion with $\mathcal{K} = \rho/\rho^0 = 2.32, \rho^0 = 2.7$ g/cm^3. The $n_f(r)$ is calculated using Kohn-Sham wave functions orthogonal to the core states and hence core-valence Pauli effects and repulsions are correctly included. The corresponding electron-ion pseudopotential $U_{ei}(k) = n_f(k)/\chi_{ee}(k,T_e)$ uses the electron-electron response function χ_{ee} at T_e. It uses a local-field correction (LFC). The LFC uses the electron compressibility κ_e matched to the finite-T exchange-correlation functional [33]. Given the pseudopotential $U_{ei}(k)$, the pair-potential is evaluated as in Ref. [29]. Thus $V_{ii}(k) = 4\pi Z^2/k^2 + |U_{ei}(k)|^2\chi_{ee}(k,T_e)$.

The real-space form $V_{ii}^{\rm NPA}(r)$ can be compared with $V_{ii}^{\rm ysrr}(r)$, where Fletcher *et al.* use the Thomsas-Fermi wavevector for Yukawa screening, with $k_s = k_{\rm TF}$. The value of σ is 4.9 a.u. correcting what may be an error in Ref. [4] where σ= 9.4 a.u. is quoted [34]. The $W(k)$ from the NPA and YSRR can be compareed with the XRTS $W(k)$. Fig. 1 shows $W(k)$ for Al, $\mathcal{K} = 2.32$, at 1.75 eV, with the $S(k)$ generated from a hyper-netted-chain (HNC) equation, i.e., without a bridge term. The Gibbs-Bogoluibov-Lado *et al.* (GBL) criterion [30, 31] for the bridge function $B(\eta, r)$ gives a hard-sphere packing fraction $\eta = 0.354$ for the modified-HNC (MHNC). The ion feature $W(k)$ from NPA-MHNC is in better agreement with experiment (Fig. 1).

The YSRR model was justified in Fletcher *et al.* and in Wunsch *et al* [20] for inverting a given $S(k)$ obtained from an MD simulation to extract a $V_{ii}(r)$ containing core-repulsion effects. The NPA calculation for Al at $T_e = 1.75$ eV, $\mathcal{K}$=2.32 shows that the mean radius of the $n = 2, l = 0$ shell in Al, reflecting the radius of the bound core is 0.3552 Å, while the YSRR potential reaches large values already by 2Å. We find that both the short-range part $\{\sigma/r\}^4$ and the long-range part $\exp(-k_s r)/r$ of the YSRR form are untenable.

The liquid-metal community of the 1980s found that the inverse problem of extracting a potential from the $S(k)$ given in a limited k-range, obtained from DFT+MD or from experiment is misleading and not unique [35, 36]. However, a parametrized physically valid model (e.g.,the model of a pair-potential $V_{ii}(r)$ constrained via an atomic pseudopotential) together with a good $B(\eta, r)$ [31] can successfully invert the MD-data. However, the DFT+MD step is quite unnecessary in most cases since the $V_{ii}^{\rm NPA}(r)$ and the $S(k)$ that provide the physics are easily evaluated from an NPA calculation.

Aluminum at $\mathcal{K} = 2.32$, $T_e = 1.75$ eV, i.e., $T_e/E_F = 0.085$, has a near-degenerate electron gas with $V_{ii}^{\rm NPA}(r)$

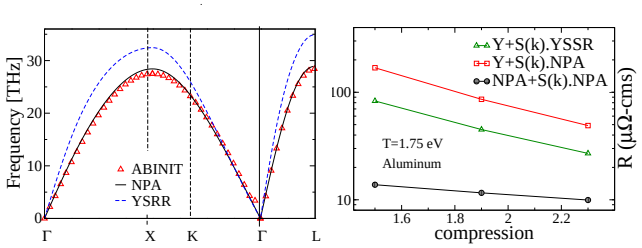

FIG. 3: (a)Longitudinal phonons of Al (T_e=1.75 eV, $\mathcal{K}$ = 2.32) from NPA, YSRR, and ABINIT. (b)Resisitivity R from Yukawa and NPA $U_{ei}(k)$ and YSSR and NPA $S(k)$.

displaying Friedel oscillations, c.f., Fig. 2(b). The $S(k)$ from the NPA-HNC, NPA-MHNC and YSRR-HNC are shown in Fig. 2(a). The NPA-HNC $S(k)$ is very similar to the YSRR-$S(k)$ but differs in the $k \to 0$ region, panel (c), and near $2k_F$. The MHNC gives a higher main peak and an improved fit to the experiment. The YSRR $S(k)$ grossly contravenes the compressibility sum rule, and a $B(\eta, r)$ would make matters worse. Hence the YSRR-$S(k)$ is only from the HNC, withpout a $B(\eta, r)$. The sum rule $S_{ii}(0) = \rho T_i \kappa$ gives the compressibility κ as 9.6 a.u. from the YSRR $S(0)$, while the NPA-HNC gives 29 a.u. and MHNC gives 26 a.u. The NPA κ is close to the the compressibility of $\sim$ 30 a.u. from an ABINIT calculation (Thus the YSRR model is not trustworthy enough for EOS properties like the compressibility.

Current XRTS spectra do not resolve the structure in $S_{ii}(\omega)$. However, this is approximated by the longitudinal-phonon spectrum which survives in the liquid state. In Fig. 3(a), we present the longitudinal phonon branch for an Al-FCC lattice at $\rho/\rho^0 = 2.32$ and T_e=1.75 eV, calculated from the NPA potential, the YSRR potential, and from an ABINIT simulation. The unphysical "stiffness" of the YSRR potential leads to high phonon frequencies and a sound velocity more than $\sim$20% greater than the NPA and ABINIT predictions.

We test the validity of the Yukawa component in the YSRR model and the validity (or not) of the YSRR-$S(k)$ by calculating the electrical resistivity R of aluminum for $1.5 < \mathcal{K} < 2.32$ at T_e=1.75 eV. The Yukawa pair-potential $Z^2 \exp(-k_s r)/r$ arises from the Yukawa pseudopotential $U^y_{ei}(q) = -Z/(q^2 + k_s^2)$ screened by the $k \to 0$ RPA dielectric function, i.e., $\epsilon(q) = 1 + (k_s/q)^2$. We use the Ziman formula given in [37], Eq. (31), with (a) NPA $S_{ii}(q)$ and the NPA pseudopotential $U_{ei}(q)$, (b) NPA $S_{ii}(q)$ with $U^y_{ei}(q)$, and YSRR $S(q)$ with $U^y_{ei}(q)$, to calculate R shown in Fig. 3(b). The NPA-$U_{ei}(q)$ used with the NPA-$S(k)$ in the Ziman formula is a well-tested method for weak scatterers [37, 38]. It shows little change in R with $\mathcal{K}$ in this highly degenerate, compressed regime, unlike the YSRR model. These results show that both the SRR potential, as well as the point-ion linear-screening (Yukawa) model are untenable. An easily computable model with the correct physics is the DFT-based NPA

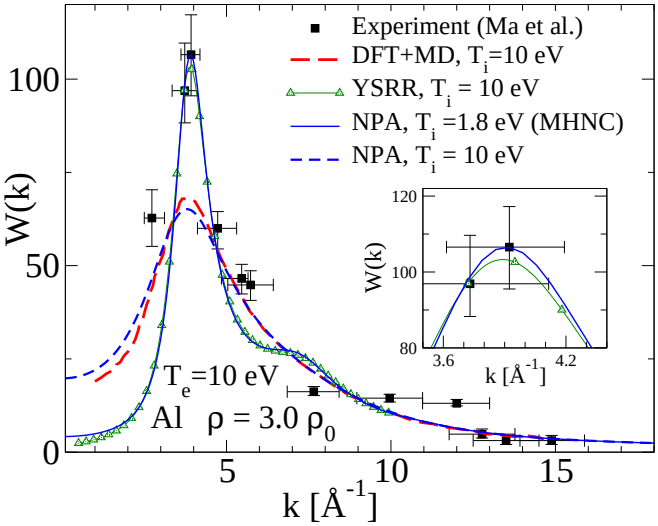

FIG. 4: XRTS ion feature $W(k)$ of Ma et al [6] is compared with the $W(k)$ from YSRR, NPA, the DFT+MD $T_i = T_e$ calculation of Rütter *et al.*, and from a $2T$-NPA calculation with T_i = 1.8 eV, T_e = 10 eV.

presented here. It generates a parameter-free simple (local) pseudopotential $U_{ei}(q) = n_f(q)/\chi(q)$.

The claim that the YSRR potential "accounts for the additional repulsion from overlapping bound-electron wavefunctions" [4] is not confirmed by the calculated atomic structure of Al^3+ in the plasma. The core-core interaction can be explicitly calculated from the core-charge density using the analysis given in Appendix B of Ref. [37]. It is quite negligible at the compressions used in Refs. [4, 6].

Study of WDM-Al by Ma et al– Ma *et al* [6] studied aluminum at $\rho/\rho^0 = 3$ and T_e=10 eV. The YSRR model with $T_i = T_e$ misleadingly showed good agreement with the experiment. Ma *et al.* state that the results from the YSRR model demonstrate the "importance of the short-range repulsion stemming from bound electrons in addition to Yukawa-type linear screening caused by the free electrons". As already noted, the core-core repulsion term in aluminum is negligible [37].

The ion feature at $T_e = T_i$ = 10 eV and $\mathcal{K} = 3$ determined by the DFT+MD simulation of Rütter *et al.*[32] disagreed with the data of Ma *et al.* 4. Using additional DFT+MD simulations, Clérouin *et al.* proposed [15] a $2T$ model where T_i = 2 eV while T_e = 10 eV. Using the NPA-potential at T_e=10 eV, and the MHNC with $\eta = 0.367$ given by the GBL criterion, we obtain an excellent fit to the Ma *et al.* data with T_i = 1.8 eV,

The high-k shoulders of the $W(k)$ from the $2T$ NPA-MHNC, and from the YSRR are washed-out in the experiment, suggesting more complexity than in a $2T$ system. The ion-subsystem may be cold (at 1.8 eV), but containing an unknown high-T component as well.

In Fig. 5, the NPA and YSRR $S(k)$, pair-potentials

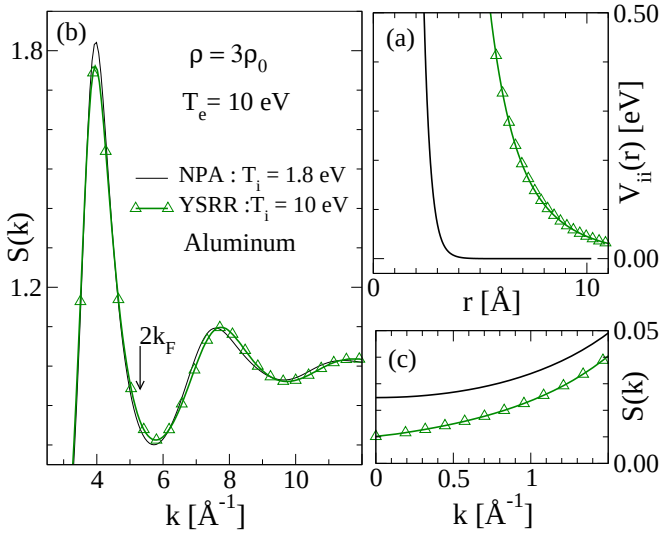

FIG. 5: (a) The NPA and YSRR pair potentials. (b) the $S(k)$ from YSRR, and NPA-MHNC (c)$S(k)$ for $k < 1.5$.

$V_{ii}(r)$ and the $k \to 0$ limit are presented in panels (a)-(c). There are no Friedel oscilaltions in $V_{ii}^{\rm NPA}(r)$ as T_e is nearly six times higher that in Fletcher *et al.*. However, assuming that $S_{ii}(k=0) = \rho T_i \kappa$ even for $2T$ systems, the YSRR model gives $\kappa = 1.06$ a.u., i.e., much lower than in the NPA result($T_i = 1.8$ eV, $T_e = 10$ eV) of 14.0 a.u., which is close to the ABINIT result of 16.4 a.u. for the $T_e = 10$ eV system.

Conclusion– The NPA model uses the electron density to obtain a a parameter-free calculations of the pseudopotentials, pair potentials, structure factors, transport coefficients, XRTS spectrum etc of a given material. We have used the NPA method to (a) investigate a popular model of a Yukawa-screened short-range-repulsive potential and shown that both its short-ranged part, as well as its screening part lead to misleading compressibilities, phonons, transport data and XRTS spectra. (b) expose pitfalls in inverting structure data to obtain effective potentials, (c) to focus on non-equilibrium states in laser-generated WDMs, and (d) present results from rapid, accurate NPA calculations.

Acknowledgments– This work was supported by grants from the Natural Sciences and Engineering Research Council of Canada (NSERC) and the Fonds de Recherche du Québec - Nature et Technologies (FRQ-NT). We are indebted to Calcul Québec and Calcul Canada for generous allocations of computer resources.

* Email address: chandre.dharma-wardana@nrc-cnrc.gc.ca

[1] G. Dimonte and J. Daligault, Phys. Rev. Lett. **101**, 135001 (2008).
[2] F. R. Graziani *et al.* Lawrence Livermore National Laboratory report, USA, LLNL-JRNL-469771 (2011).
[3] P. Lorazo, L. J. Lewis, and M. Meunier, Phys. Rev. Lett. **91**, 225502 (2003); Phys. Rev. B **73**, 134108 (2006).
[4] L. B. Fletcher *et al*, Nature Photonics **9**, 274 (2015).
[5] E. García Saiz *et al*, Nature **4** (2008).
[6] T. Ma *et al*, Phys. Rev. Lett. **110**, 065001 (2013).
[7] H. M. Milchberg *et al*, Phys. Rev. Lett. **61**, 2364 (1988).
[8] Z. Chen, B *et al*, Phys. Rev. Lett. **110**, 135001 (2013).
[9] P. Sperling et al., Phys. Rev. Lett. **115**, 115001 (2015).
[10] Medvedved *et al*, Phys. Rev. Lett. **107**, 165003 (2011).
[11] M. W. C. Dharma-wardana, Phys. Rev. E **64**, 035432(R) (2001).
[12] S. I. Anisimov *et al*, Sov. Phys. JETP 39, 375 (1974).
[13] M. W. C. Dharma-wardana, arXiv:1602.04734 (2016).
[14] K. Plagemann *et al*, Phys. Rev. E **92**, 013103 (2015).
[15] J. Clérouin *et al*, Phys. Rev. E **91** 011101(R) (2015).
[16] G. Kresse and J. Furthmmüller, Phys. Rev. B **54**, 11169 (1996);
[17] X. Gonze *et al*, Comp. Phys. Com. **180**, 2582-2615 (2009).
[18] M. W. C. dharma-wardana, and François Perrot, Phys. Rev. E **58**, 3705-3718 (1998)
[19] M. W. C. Dharma-wardana, Phys. Rev. E **64** 035432(R) (2001)
[20] K. Wunsch *et al*, Phys. Rev. E **79**, 010201 (2009).
[21] S. H. Glenzer and R. Redmer, Rev. Mod. Phys. **81**, 1625 (2009).
[22] G. Gregori *et al*, Phys. Rev. E **74** 026402 (2006).
[23] L. Dagens, J. Phys. C **5**, 2333 (1972); L. Dagens, J. Phys. (Paris) **36**, 521 (1975).
[24] M. W. C. Dharma-wardana and F. Perrot, Phys. Rev. A **26**, 4 (1982).
[25] F. Perrot, Phys. Rev. E **47**, 570 (1993).
[26] C. E. Starrett and D. Saumon, Phys. Rev. E **92**, 033101 (2015); Wilson et al., JQSRT **99**, 658-679 (2006); R. Piron and T. Blenski Phys. Rev. E **83**, 026403, (2011); M. S. Murillo, *et al*, Phys. Rev. E **87**, 063113 (2013).
[27] F. Perrot and M.W.C. Dharma-wardana, Phys. Rev. E. **52**, 2920 (1995); M. W. C. Dharma-wardana, Cont. Plas. Phys. **55** 97 (2015).
[28] L. Harbour *et al*, Contr. Plasma. Phys. **55**, 144 (2015)
[29] M. W. C. Dharma-wardana, Phys. Rew. E **86**, 036407 (2012)
[30] F. Lado *et al.* Phys. Rev. A **28**, 2374 (1983).
[31] H. C. Chen Phys. Rev. A **45**, 3831 (1991)
[32] H. K. Rüther and R. Redmer, Phys. Rev. Lett. **112**, 145007 (2014)
[33] F. Perrot and M. W. C. Dharma-wardana, Phys. Rev. B **62**, 16536 (2000); *Erratum:* **67**, 79901 (2003); arXive-1602.04734 (2016).
[34] We have contacted the authors of Ref. [4] regarding this. If $\sigma = 9.4$, then the classical coupling constant at $r_{\rm ws} = 1$ a.u. would be over 7800 at all temperatures as this term is independent of T. The HNC does not converge for $\sigma \sim 9$, although it may be treated using MD.
[35] N. H. March, Canadian Journal of Physics, **65** 219-240, (1987)
[36] M.W. C. Dharma-wardana and G. C. Aers. Phys. Rev. B, **28**, 1701 (1983); Phys. Rev. Lett. **56**, 121 (1986).
[37] François Perrot et al, Phys. Rev E **52** 5352 (1995)
[38] J. Benage *et al.*, Phys. Rev. Lett. **83**, 2953 (1999)